2022 7th IEEE International Conference on
Advanced Robotics and Mechatronics
July 9-11, 2022, Guilin, China

2022 International Conference on Advanced Robotics and Mechatronics (ICARM) | 978-1-6654-8306-3/22/$31.00 ©2022 IEEE | DOI: 10.1109/ICARM54641.2022.9959370

A Hybrid Wheel-Leg Transformable Robot with Minimal Actuator Realization

Zhengtao Liu, Cunxi Dai, Xiaohan Liu, Jianxiang Zhou, and Zhenzhong Jia

***Abstract*—Wheel-leg transformable robots have great overall performance in various terrains by taking full advantage of both locomotion modalities. However, they tend to have much more complicated designs and actuators than single-mode robots. This paper proposes a wheel-leg transformable robot design with minimal actuator realization. To this end, we design a novel wheel-leg transformable module that uses tendon-driven mechanism for motion mode switching of each module, and a tendon network that uses a single actuator to control all tendons for mode switching of the entire robot. Hence, a N-legged robot only needs $N + 1$ actuators. To validate our design, we build an experiment platform, develop associated control algorithms, and conduct both simulation and field experiments over flat ground and rough terrains such as stairs and obstacles.**

I. Introduction

Wheeled and legged mobile robots are still the most popular form of ground mobile robots during the development of robotics. Our environment can be roughly divided into flat and rough terrains [1]. Wheels and legs have their respective unique characteristics over these two specific types of terrains. In general, wheels have great performance on flat ground, such as high speed, stability, and efficiency; however, they will have poor mobility when facing rough terrain, resulting in slippage or even immobility [2]. In contrast, legged robots have extraordinary mobility over rough terrain, although they cannot compete with wheeled robots on flat ground in terms of speed and efficiency [3]. Therefore, wheel-leg transformable robots that can combine the advantages of both locomotion modalities will likely have the best overall performance in various environment conditions [1], [4].

There are some wheel-leg transformable robots reported in the literature [5], [6], [1]. Some wheel-leg robots such as those in [7], [8] select "search and rescue" as their main tasks. These working environments are highly dangerous and are likely to pose a major threat to human life. These working environments often have diverse terrains, requiring robots to have high-speed mobility over different types of terrains in order to complete the tasks in a timely manner because of the urgent nature of these tasks. Note that crawlers and legged robots have good all-terrain mobility; however, their flat ground speed cannot match wheeled robots. In comparison, wheel-leg transformable robots that can switch to suitable motion modes (i.e., wheeled mode over flat ground, legged mode in rough terrain) can be very competitive in such tasks [9].

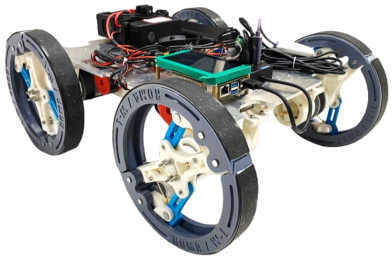

Fig. 1. Our proposed wheel-leg transformable robot with minimal actuators

The great overall performance of wheel-leg transformable over different terrains comes with a price, i.e., system complexity. They are much more complicated than robots with a single locomotion modality. Moreover, they often have much more actuators, which can significantly increase the system cost. For example, the hexapod Slegs robot reported in [5] has at least 18 actuators, i.e., 3 actuators for each wheel-leg module. Slegs robot uses 6×1 main actuators to drive the 6 wheel-leg modules and additional 6×2 actuators (servos or linear actuators) to switch between the wheel and leg modes. The Quattroped robot in [6] and the turboquad robot in [1] are both quadruped robots with at least 8 actuators. The turboquad robot uses 4×2 main actuators to drive the specially-designed wheel-leg module, which can complete mode switching online. It also uses an additional actuator to control the Ackermann steering mechanism. Hence, it has 9 actuators in total. To our best knowledge, all wheel-leg transformable robots reported in the literature with N wheel-leg modules will have at least $2N$ actuators.

In this paper, we propose a wheel-leg transformable robot design with minimal actuator realization, as shown in Fig. 1. In particular, for a robot with N wheel-leg modules, we only need $N + 1$ actuators. This is only about 50% of literature designs. This will help reduce the system complexity, cost, and failure rate. The main contributions are:

1) We propose a robot design that can perform wheel-leg switching using minimal actuator realization. In par-

All authors are with the Shenzhen Key Laboratory of Biomimetic Robotics and Intelligent Systems, Department of Mechanical and Energy Engineering, Southern University of Science and Technology (SUSTech), Shenzhen, 518055, China. They are also with Guangdong Provincial Key Laboratory of Human-Augmentation and Rehabilitation Robotics in Universities, SUSTech, Shenzhen, 518055, China. *Corresponding author: jiazz@sustech.edu.cn

ticular, the N-legged robot only needs $N+1$ actuators, with only one actuator for mode switching. This can greatly reduce the actuator number and system cost.

2) We design a novel wheel-leg transformable module that uses a tendon-driven mechanism for locomotion mode switching. We also propose a design that can use a single actuator to control all tendons to finish mode switching of the entire robot.
3) We build a mechatronics experiment platform to validate our design. We also develop control algorithms for the new robot and conduct both simulation and field experiments to test the effectiveness of our design.

II. Robot Design

The online wheel-leg transformation during walking is accomplished by a transformation mechanism that includes a tendon-driven leg–wheel switching mechanism, wheel-leg module, and the corresponding driving mechanism, as shown in Fig. 2. The four leg–wheel switching mechanisms are driven by a single servo and are therefore synchronized, but the rotation of each is driven by four motors separately. To further investigate the performance of a quasi-wheel-leg robot, we used two servos to drive the transformation mechanism of the front wheels and back wheels separately. However, the feasibility of using only one servo is already validated in the second part of this section.

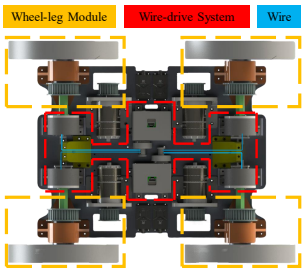

Fig. 2. Two modules in the whole robot

A. Design of Overall System

The tendon-driven transformation mechanism is driven by two servos placed at the geometric center of the robot's orthographic projection, which drives the transformation of the front and back wheel-leg module separately. Pulleys on the desired pathway to guide the tendons, the bottom-view of the robot is shown in Fig. 2. Each wheel-leg module is driven by one motor with a belt transmission system comprising two pulleys and a timing belt with a 22:34 speed reduction. A rotating connector is placed directly behind the wheel to prevent tendon twisting between the rotating wheel-leg and the stationary body. The rotation connector consists of a slider that moves along the axial direction of the wheel and a rotational unit, which is concentric with the wheel and fixed to the slider. The tendon first pulls on the base of the connector and causes the connector to slide on the rail. The rotational part pulls the tendon on the wheel-leg module and causes transformation while rotating with the wheel to prevent twisting. The details of the rotating connector are shown in Fig. 3.

B. Four-Bar Transformation Mechanism of the Wheel-Leg Module

One of the key requirements for the transformation mechanism is the stability to maintain the legged mode without over-driving the servo. Based on this, we designed a single-DOF four-bar mechanism that reaches singularity when fully transformed into legged mode. The wheel-leg module consists of two symmetrical four-link transformation units; both have one link being the central rod, intermediate rods (Rod1, Rod2), and spokes (Spoke) fixed partially to the mechanism, and the model diagram of the wheel-leg deformation mechanism is shown in Fig. 3.

Two main principles should be followed when selecting the design parameters for the wheel-leg transformation mechanism. The first is that the wheel-leg module can deform as much as possible in the leg mode, and this module has as large a region of elasticity(AB) as possible. Another principle is that the wheel-leg module uses the mechanism singularity to reduce the impact on the servo when trotting in legged mode and the stall-mode energy consumption of the transformation servo[10]. Hence, the following constraints are defined:

1) The wheel-leg module has the largest possible elastic area in the leg mode. Therefore, arc BC in Fig. 3 is as short as possible without causing structural interference.
2) Use the singularity of the four-link mechanism in the leg mode to reduce the requirements for wire tension.
3) Interference between the components during deformation must be avoided.
4) In the leg mode, Rod1 and Rod2 in Fig. 3 will be in the singular position to reduce the requirements for wire tension.

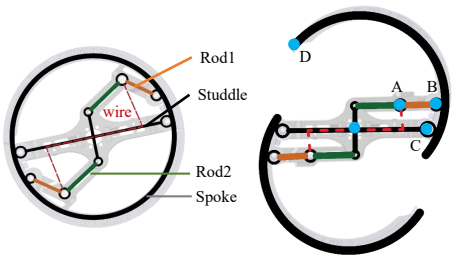

(a) Wheel mode (b) Leg mode

Fig. 3. The schematic diagram of a wheel-leg module in two modes

We set up the simulation in MATLAB to find the parameters of the four-link mechanism satisfying the four constraints mentioned above. Fig. 3 shows the schematic diagram of

the two modes of the wheel-leg module with the optimal parameters. When transforming from wheel mode, the tendon-driven system pulls the tendon in order to pull on joint B and bring the deformation mechanism to the mechanical limit (four-link singularity) shown as Fig. 3(b) and keep the tension. When restoring, the servo reverses to release the tension, and the torsion spring installed at joint C provides the torque to restore the wheel mode. Besides, to reduce the friction acting on the tendon, pins and pulleys are embedded in the center rod to smooth the process.

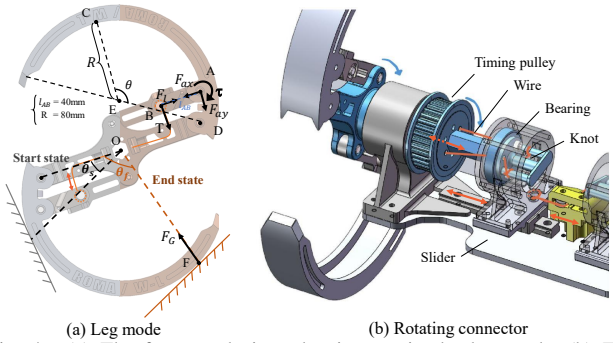

(a) Leg mode (b) Rotating connector

Fig. 4. (a) The force analysis and gait state in the leg mode. (b) The winding rotating connector schematic, blue arrows mark the direction of wheel rotation, orange mark the direction of rope drive movement.

In order to select a proper servo for the transformation system, we analyzed the required torque to maintain legged mode. We are assuming that the robot moves slowly enough. The acceleration and angular acceleration are both nearly zero. Under this assumption, the force analysis of the isolated linkage in the leg mode is shown in Fig. 4. From the force analysis for Rod1 in the leg fully open state, because the angular acceleration is assumed to be zero, the interaction force between Rod1 and Rod2 is along the direction of the rod. The force analysis on Rod2 gives the following equation:

$$Tl_{AB} = \tau \tag{1}$$

where T is the tension of the line at point B, approximated as the vertical direction along the rod, $l_{AB} = 40mm$ is the length of rod2, and τ is the torque of the torsion spring.

The effect of torsion spring is to transform the leg mode to wheel mode. According to the experiment tests, we choose a torsion spring which completes switching function, and the torsion spring constant $k = 0.43274Nm/rad$. And the maximum turning angle of the torsion spring is $\alpha = 1.9247rad$ in the leg mode of the Fig. 4. And the outer diameter of the winch is $d = 10.5mm$, and the deformation motor needs to drive 4 degenerate mechanisms of 4 wheel-leg modules at the same time.

$$\tau = k\alpha, \tau_{servo} = 4Td \tag{2}$$

The minimum torque is $\tau_{servo} = 0.8746Nm$. The servo chose is Feetech's SMS series serial RS485 bus servo, which can provide a maximum continuous torque of $2.8Nm$, which is sufficient to support the robot to keep its leg mode.

TABLE I
ROBOT SPECIFICATIONS

Length	Body	0.4m
	Hip-to-hip	0.3m
Width	Body	0.3m
	Leg-to-leg	0.39m
Height	Body	0.154m
	Ground to hip (legged mode)	0.0965m
	Ground clearance (legged mode)	0.193m
Leg–wheel (i.e., rim) diameter		0.0965m
Maximum radius of leg–wheel		0.1250m
Weight	Total	8.406kg
	Body	6.392kg
	Leg-wheel(each)	0.336kg
	Battery	0.673kg
Actuator	Driving	Dji M3508 motor(×8)
	Switch mechanism	Feetech SMS serial servo(×2)
Sensors	Encoder	(×4)@motor
	Temperature sensor	(×1)@computing unit
	Current measurement	(×1)@motor power output
	Battery voltage measurement	(×1)@power output
Battery	Dji TB48	30 min continuous run time

III. MECHATRONIC SYSTEM

The main computation power on this robot is the Raspberry Pi 4B embedded computer, Robot Operating System(ROS) is used on this board for inter-module communication.

4 Dji M3508 brushless geared motors are used as the major power unit for this robot. Each motor is connected to a Dji C620 FOC controller. The controllers accept the current command and provide current, speed, and position feedback. A socketcan board that converts the CAN signal to a USB signal is used to connect the FOCs and the embedded computer. Two Feetech SMS serial servos were used to power the tendon-driven system. The servos are connected to a driver board which provides power and signal exchange. The driver board is also connected to the embedded computer. The specifications of the robot are summarized in Table I.

IV. CONTROL AND SIMULATION

The robot has two different control modes: wheeled mode and legged mode. Both modes can be adapted to wheel-leg transformable robots with 6 or more wheel-leg modules with minor modifications as the principles of control remains the same. Our modulated design principle also facilitates this process, which we will dig deeper into the upcoming research.

A. Wheeled Mode

When the robot operates in wheeled mode, the control of the joints is straightforward. The rotation speeds (ω_i) of each joint are assigned based on the differential-wheel steering model. Wheels on the same side of the robot will be assigned the same angular velocity, ω_L or ω_R.

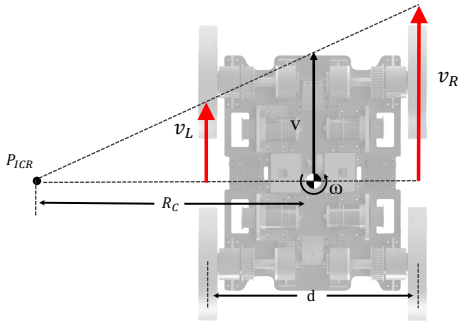

Fig. 5. Differential-wheel steering when operated in wheeled mode

As shown in Fig. 5, when the robot has a forward velocity v and a rotational velocity ω, its instant center of rotation will be located at point P_{ICR}. The turning radius can be expressed as:

$$R_c = \frac{V}{\omega}$$

Then, the angular velocity of each joint can be computed as

$$w_{RF} = w_{RB} = \frac{V + \frac{\omega d}{2}}{R_{wheel} N_t}$$

$$w_{LF} = w_{LB} = \frac{V - \frac{\omega d}{2}}{R_{wheel} N_t}$$

where d is the width of the chassis and N_t is the speed reduction ratio. The motions are shown in Fig. 9. This control strategy can be also used in robots with more wheel-legs.

B. Legged Mode

For leg mode, a simple Rhex-like control strategy is implemented ref[11]. This control strategy is joint space close-loop but task space open loop. Once given the target gait and speed, the algorithm will generate a group of clock-driven trajectories for each joint. The trajectories will then be tracked by cascaded PD joint controllers.

The trajectory generated is a periodic function of time which has an output ranging from 0 to π. The trajectory has four key parameters: θ_s, θ_f, t_s and t_c. t_c and t_s will determine the duty factor of each leg. The period of the function is t_c. θ_s and θ_f are threshold for gait control. The leg approximately hits the ground when $\theta = \theta_s$ and leaves the ground when $\theta = \theta_f$. The speed provided by each leg during its stance phase is approximately

$$V_{leg} = \frac{(R(\theta_f) - R(\theta_s))(\theta_f - \theta_s)}{2(T_f - T_s)}$$

where $R(\theta)$ is the estimated length between the contact point and the joint.

As shown in Fig. 5(a), there are phase differences t_k between the trajectories of the different legs. The phase differences are determined by the robot's configuration and gait.

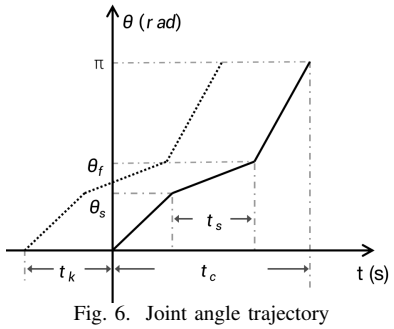

Fig. 6. Joint angle trajectory

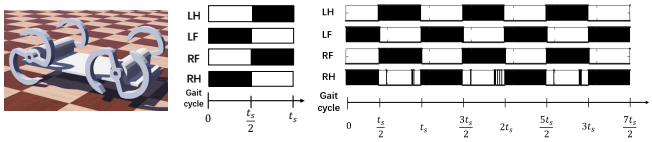

(a) Trot gait (b) Designed trot gait (c) Trot gait in simulation

Fig. 7. (a) The trot gait simulation of quadruped robot in webots. (b) Designed trot gait diagrams and (c) The simulation result. The black and white sections represent the stance phase and the aerial phase, respectively.

The leg-mode control strategy is tested in simulation on a simplified robot model. The collision data of the leg is collected and used as the ground truth of actual gait. Fig. 7(b)(c) shows that the actual gait is basically consistent with the designed gait.

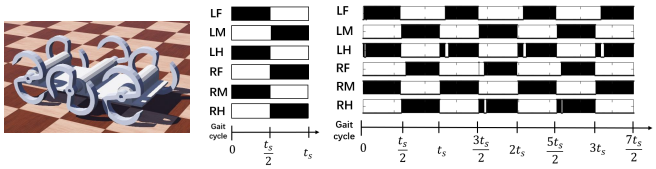

(a) Triangular gait (b) Designed triangular gait (c) Triangular gait in simulation

Fig. 8. (a) The tripod gait simulation of hexapod version robot in webots. (b) Designed tripod gait diagrams and (c) the simulation result. The black and white sections represent the stance phase and the aerial phase, respectively.

This control strategy can also be easily transferred to robots that have more wheel-legs. Fig. 8 shows the gait simulation result of the hexapod version of our robot. The six-leg version robot walks more smoothly due to the intrinsic stability property of hexapod robots.

V. Experiments

A. Control of Tendon-driven System

The nonlinear properties of the tendon and the multi-DOF mechanism make the control of our wire-drive system to be difficult. In this experiment, the accurate mapping between the servo rotation angle and the distance CD is shown in Fig. 11 which is measured to ensure precise control over the transformation process.

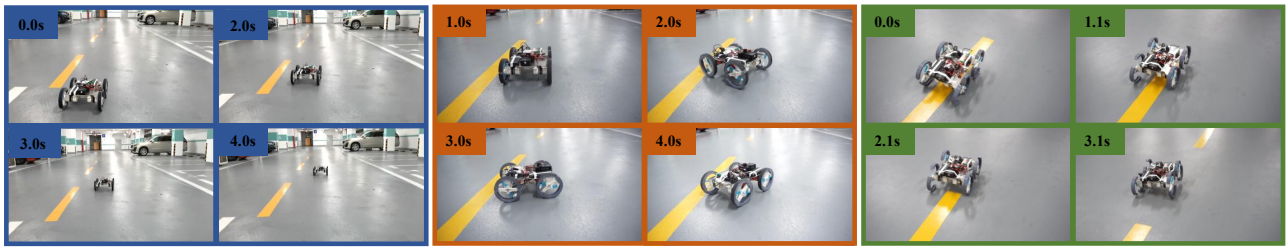

a) Straight walking in wheel mode b) Rotation in wheel mode c) Straight walking in leg mode

Fig. 9. Motion for the wheel-leg transformable robot

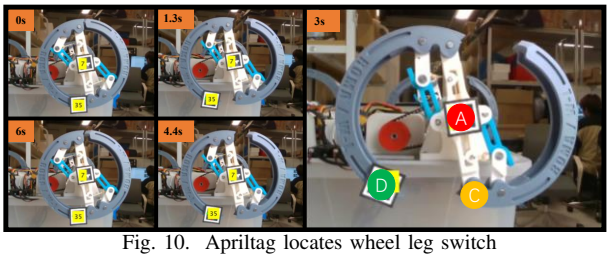

Fig. 10. Apriltag locates wheel leg switch

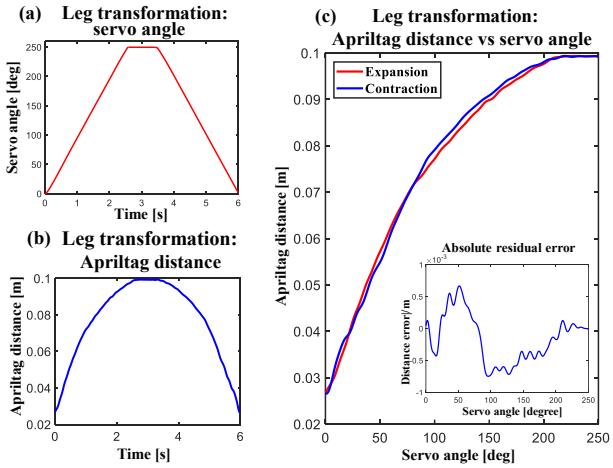

Fig. 11. (a) The change of the rotation angle of the steering gear with time during the test process. (b) The change of distance between CD measured by Apriltag. (c) The mapping relationship between rotation angle of the steering geer and distance between CD.

The rotational angle can be directly obtained from the built-in encoder of the servo. The distance AD is identified by Apriltag. As shown in Fig. 10, we place the Apriltag QR code at points A and D, then use the calibrated camera to take pictures and calculate the spatial position (x, y, z) of the two points A and D with respect to the camera coordinate system in the real world and calculate the distance AD. Then we can solve for the distance CD via geometric constraints . Therefore, by recording the switching process of the wheel-leg, we can precisely map between the servo rotation angle and the distance CD.

Fig. 10 shows the switching process schematic diagram of the wheel-leg module first from wheel mode to leg mode, and then from leg mode to wheel mode. Fig. 11(a) is the servo angle with respect to time in the switching process of two motion mode. Fig. 11(b) is the change of distance CD with time. Fig. 11(c) is the change of distance CD with respect to servo angle, where two lines correspond to the mapping of the extension and retraction of the wheel-leg module respectively. The error of two switching process is shown at the bottom-right corner of Fig. 11(c) and the transformable process has the low hysteresis.

B. Power Consumption on Even Terrain

The performance of power consumption was evaluated using specific resistance (SR). [1].

$$SR = \frac{P}{mgv} \tag{3}$$

where m is the mass of the system, P is the power consumption, and v is the average forward speed. The total power consumption includes the power from all motors but neglects the power from the processors.

We tested the power consumption under v = 0.5 m/s. At this speed, SR value is 0.813 in wheeled mode and 2.2374 in legged mode. It can be noticed that the power efficiency of wheeled mode is much higher than the efficiency of legged mode. This phenomenon meets general expectations: in legged mode, the frequent joint acceleration and deceleration will consume extra energy. So when the terrain is even, wheeled mode is a more energy-efficient choice.

C. Stair Climbing Experiment

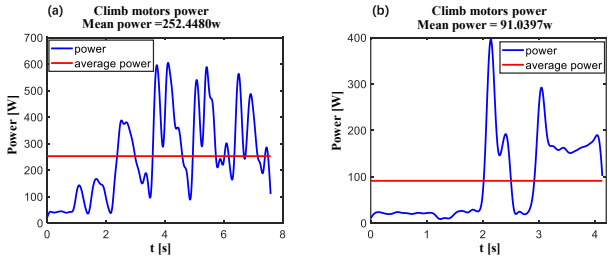

Fig. 12. Motor current diagram for upstairs experiment

As a mobile robot, our robot should be able to move or steer in different terrain [12]. Usually, wheeled robots have limited passability on uneven terrain. In this test, we tested our robot on stairs with a naive stair-climbing algorithm, in

which the two front joints and the two rear joints are coupled separately [13]. Theses two tests demonstrate that the legged mode of the robot has superior passability on uneven terrains compared to wheeled mode.

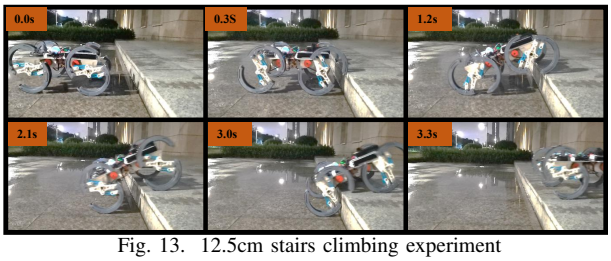

Fig. 13. 12.5cm stairs climbing experiment

The robot is tested on two different set of stairs. The first stair we tested is 12.5cm tall, as shown in Fig. 13, which is higher than our platform height and the wheel radius. Fig. 12(a) demonstrates the total power consumption of four motors of the robot when climbing the stairs. The first peak in this graph appears when the front legs are in contact with the stairs, and the second peak appears when the back legs are in contact.

The second group of stairs consists of multiple stairs, as shown in Fig. 14. Each of the stairs has a height of 7 cm, which is lightly lower than the radius of the wheel radius. Fig. 12(b) shows the power consumption in this test.

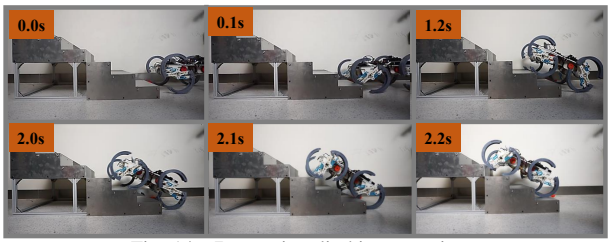

Fig. 14. 7cm stairs climbing experiment

VI. Conclusion and Future Work

This paper proposes a wheel-leg transformable robot design with minimal actuator realization. We only use about 50% actuators when compared to the literature designs. This greatly reduces system complexity, cost, and failure rate. The proposed design has a novel wheel-leg transformable module that uses tendon-driven for motion mode switching and a tendon network that uses a single actuator to switch the motion mode of the entire robot. We conduct both simulation and field experiments to validate our design. Our robot shows great mobility and obstacle negotiation capability. In the future, we will further improve the design, making the system more reliable and easy to configure. We will also test the Rhex-like hexapod design for more stable gaits and use the camera to do the motion planning [14].

Acknowledgments

This work was supported in part by the Science, Technology and Innovation Commission of Shenzhen Municipality under grant no. ZDSYS20200811143601004.

References

[1] W.-H. Chen, H.-S. Lin, Y.-M. Lin, and P.-C. Lin, "Turboquad: A novel leg–wheel transformable robot with smooth and fast behavioral transitions," *IEEE Transactions on Robotics*, vol. 33, no. 5, pp. 1025–1040, 2017.

[2] Y.-S. Kim, G.-P. Jung, H. Kim, K.-J. Cho, and C.-N. Chu, "Wheel transformer: A wheel-leg hybrid robot with passive transformable wheels," *IEEE Transactions on Robotics*, vol. 30, no. 6, pp. 1487–1498, 2014.

[3] R. Cao, J. Gu, C. Yu, and A. Rosendo, "Omniwheg: An omnidirectional wheel-leg transformable robot," *arXiv preprint arXiv:2203.02118*, 2022.

[4] T. Sun, X. Xiang, W. Su, H. Wu, and Y. Song, "A transformable wheel-legged mobile robot: Design, analysis and experiment," *Robotics and Autonomous Systems*, vol. 98, pp. 30–41, 2017.

[5] S. Soyguder and W. Boles, "Slegs robot: development and design of a novel flexible and self-reconfigurable robot leg," *Industrial Robot: An International Journal*, vol. 44, pp. 377–391, 2017.

[6] S.-C. Chen, K.-J. Huang, W.-H. Chen, S.-Y. Shen, C.-H. Li, and P.-C. Lin, "Quattroped: a leg–wheel transformable robot," *IEEE/ASME Transactions On Mechatronics*, vol. 19, no. 2, pp. 730–742, 2013.

[7] D. Campbell and M. Buehler, "Stair descent in the simple hexapod'rhex'," *2003 IEEE International Conference on Robotics and Automation*, vol. 1, pp. 1380–1385, 2003.

[8] E. Moore, D. Campbell, F. Grimminger, and M. Buehler, "Reliable stair climbing in the simple hexapod 'rhex'," *2002 IEEE International Conference on Robotics and Automation*, vol. 3, pp. 2222–2227, 2002.

[9] K. Tadakuma, R. Tadakuma, A. Maruyama, E. Rohmer, K. Nagatani, K. Yoshida, A. Ming, M. Shimojo, M. Higashimori, and M. Kaneko, "Mechanical design of the wheel-leg hybrid mobile robot to realize a large wheel diameter," *2010 IEEE/RSJ international conference on intelligent robots and systems*, pp. 3358–3365, 2010.

[10] S.-C. Chen, K.-J. Huang, W.-H. Chen, S.-Y. Shen, C.-H. Li, and P.-C. Lin, "Quattroped: A leg–wheel transformable robot," *IEEE/ASME Transactions on Mechatronics*, vol. 19, no. 2, pp. 730–742, 2014.

[11] U. Saranli, M. Buehler, and D. E. Koditschek, "Design, modeling and preliminary control of a compliant hexapod robot," *IEEE International Conference on Robotics and Automation.*, vol. 3, pp. 2589–2596, 2000.

[12] J. Li, J. Wang, H. Peng, Y. Hu, and H. Su, "Fuzzy-torque approximation-enhanced sliding mode control for lateral stability of mobile robot," *IEEE Transactions on Systems, Man, and Cybernetics: Systems*, vol. 52, pp. 2491–2500, 2021.

[13] S. Wang, Z. Chen, J. Li, J. Wang, J. Li, and J. Zhao, "Flexible motion framework of the six wheel-legged robot: Experimental results," *IEEE/ASME Transactions on Mechatronics*, vol. 27, pp. 2246–2257, 2021.

[14] J. Li, H. Qin, J. Wang, and J. Li, "Openstreetmap-based autonomous navigation for the four wheel-legged robot via 3d-lidar and ccd camera," *IEEE Transactions on Industrial Electronics*, vol. 69, no. 3, pp. 2708–2717, 2021.